Needle-free delivery of macromolecules across the skin by nanoliter-volume pulsed microjets

Anubhav Arora*, Itzhak Hakim†, Joy Baxter‡§, Ruben Rathnasingham†, Ravi Srinivasan†, Daniel A. Fletcher¶, and Samir Mitragotri*‡‖

*Biomolecular Science and Engineering and ‡Department of Chemical Engineering, University of California, Santa Barbara, CA 93106; ¶Department of Bioengineering, University of California, Berkeley, CA 94720-1762; and †StrataGent Life Sciences, Inc., Los Gatos, CA 95030

Needle-free liquid jet injectors were invented >50 years ago for the delivery of proteins and vaccines. Despite their long history, needle-free liquid jet injectors are not commonly used as a result of frequent pain and bruising. We hypothesized that pain and bruising originate from the deep penetration of the jets and can potentially be addressed by minimizing the penetration depth of jets into the skin. However, current jet injectors are not designed to maintain shallow dermal penetration depths. Using a new strategy of jet injection, pulsed microjets, we report on delivery of protein drugs into the skin without deep penetration. The high velocity (v >100 m/s) of microjets allows their entry into the skin, whereas the small jet diameters (50–100 μm) and extremely small volumes (2–15 nanoliters) limit the penetration depth ($\approx$200 μm). In vitro experiments confirmed quantitative delivery of molecules into human skin and in vivo experiments with rats confirmed the ability of pulsed microjets to deliver therapeutic doses of insulin across the skin. Pulsed microjet injectors could be used to deliver drugs for local as well as systemic applications without using needles.

MEMS | nanotechnology | noninvasive | piezoelectric | transdermal

H ypodermic needles are the most common mode of delivering macromolecules in humans. Currently, $\approx$12 billion needle injections are performed every year for the delivery of vaccines and protein therapeutics such as insulin, growth hormones, and erythropoietin. Needles, although effective, lead to severe issues such as pain, needle phobia, and accidental needlesticks (1). Although pain and needle phobia lead to noncompliance, accidental needlesticks lead to injuries and possible infections. Hence, there is a strong interest from the patients, healthcare providers, and drug manufacturers to develop needle-free methods of drug delivery. This, in turn, has induced significant interest in the scientific community about needle-free drug delivery. Needle-free delivery of vaccines has already been identified as one of the grand challenges in global health (2) and a priority in general (3).

Motivated by the limitations of injections, needle-free liquid jet injectors were invented more than 50 years ago (4) and have been used for delivering several vaccines and protein drugs. More recently, a number of other technologies have also been proposed to deliver proteins across the skin without using needles (5–13). These technologies are at varying degrees of development. As of today, however, liquid jet injectors comprise the only needle-free tool in the hands of clinicians for delivery of proteins and other macromolecules. Commercially available liquid jet injectors use compressed gas or a spring to create high-pressure jets of drug solutions that deliver drugs in the s.c. or i.m. region (14, 15). Despite their long history, needle-free liquid jet injectors have been met with disappointing acceptance as a result of frequent bruising and pain (4), which immediately offset their advantages against needles. We hypothesized that pain and bruising originate from deep penetration of jets into skin leading to their interactions with nerves and blood capil-

laries. This issue could potentially be addressed by minimizing the penetration depth of jets into the skin; however, attempts to reduce the penetration depth have led to a concurrent loss of delivery efficiency (16). Decoupling penetration depth and delivery efficiency has been difficult as a result of the very design of conventional jet injectors. We overcame this issue by adopting a new strategy of jet injection, pulsed microjets. We propose the use of high-velocity microjets (v >100 m/s) to ensure skin penetration but small jet diameters (50–100 μm) and extremely small volumes (a few nanoliters) to limit the penetration depth. We describe a microjet device that meets these criteria and demonstrate its capabilities by using insulin as a model drug.

Results and Discussion

Microjets were produced by displacing the drug solution through a micronozzle (50–100 μm in final diameter) by using a piezoelectric transducer (Fig. 1a). Other modes of fluid displacement, including dielectric breakdown and electromagnetic displacement, can also be potentially used (17, 18); however, the piezoelectric-based mechanism was preferred as a result of its robustness and energy efficiency. The piezoelectric transducer, on application of a voltage pulse, expands rapidly to push a plunger that ejects the fluid from the micronozzle as a high-speed microjet. The volume of the microjet is proportional to the amplitude of the voltage pulse (Fig. 2a; measured with a colorimetric assay) and the velocity of the microjet is proportional to the rise time. Ideally, a rise time of 10 μs would lead to a mean velocity of 127 m/s for a 10-nanoliter microjet delivered from a 100-μm diameter micronozzle ($v = Q/At$, where Q is the microjet volume, A is the cross-sectional area of the micronozzle, and t is the rise time). This predicted velocity compared well with the experimental value measured with strobe microscopy (see Materials and Methods). Formation of microjets was confirmed by using high-speed photography and strobe microscopy (data not shown). By controlling the amplitude and rise time of the pulse, velocity as well as volume of the microjet could be adjusted. Dispensed volume from the nozzle is replaced by liquid from the reservoir, which is maintained under slight positive pressure to avoid backflow.

Under typical operating conditions used in this study, microjets were ejected from the micronozzle at exit velocities exceeding 100 m/s and volumes of 10 to 15 nanoliters. The microjets were cylindrical in shape and each jet pulse could be clearly distinguished. To deliver volumes in excess of 10 to 15 nanoliters, the microjets were created over a prolonged period and the total

APPLIED BIOLOGICAL SCIENCES

Microjet Injector

Conventional Jet Injector

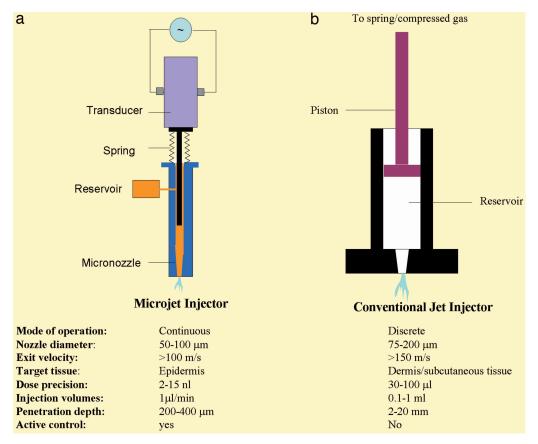|	Microjet Injector	Conventional Jet Injector
Mode of operation:	Continuous	Discrete
Nozzle diameter:	50-100 μm	75-200 μm
Exit velocity:	>100 m/s	>150 m/s
Target tissue:	Epidermis	Dermis/subcutaneous tissue
Dose precision:	2-15 nl	30-100 μl
Injection volumes:	1μl/min	0.1-1 ml
Penetration depth:	200-400 μm	2-20 mm
Active control:	yes	No

Fig. 1. Schematic of a pulsed microjet device and conventional jet injector. (*a*) A pulsed microjet injector comprises a custom-made acrylic micronozzle with final internal diameter in the range of 50–100 μm into which a stainless steel plunger is placed. The plunger is connected to a piezoelectric crystal, which is activated by a custom-designed pulse generator. Activation of the piezoelectric crystal pushes the plunger forward, thereby creating a microjet. Deactivation of the crystal moves the plunger back, and the liquid from the reservoir replenishes displaced liquid. (*b*) A conventional jet injector comprises a plastic nozzle into which a plunger is placed. The plunger is connected to a compressed spring or compressed gas chamber. Release of compressed spring or gas pushes the plunger to generate a jet. Most commercially available jet injectors are single-use devices (disposable, single-use nozzles attached to a nondisposable device). Typical operating parameters for both types of injectors are listed for the purpose of comparison.

amount of liquid ejected was proportional to the application time (Fig. 2*b*; determined with a radiolabeled tracer). For data in Fig. 2*b*, a pulsation frequency of 1 Hz (1 microjet per second) was used. This frequency could be increased if higher delivery rates are desired.

To study the penetration of microjets into a solid substrate such as skin, a model material, agarose gel, was used. The gel offers an ideal test bed because it can be produced with controllable mechanical properties and its transparency allows direct visualization of microjet penetration. Microjets readily penetrated into agar gel (Fig. 3*a*). Penetration of a single microjet is difficult to visualize as a result of small volumes and shallow penetration depths. However, the penetration depth increased with increasing number of pulses and can be clearly seen in Fig. 3*a*. The penetration depth is established very early during the injection and stabilizes at a few millimeters after five
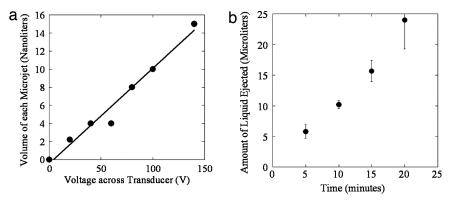

Fig. 2. Performance characteristics of the pulsed microjet injector. (*a*) Dependence of microjet volume on voltage applied across the piezoelectric crystal. A microjet volume of 15 nl was used for most experiments reported in this study. (*b*) Dependence of total microjet volume ejected in air as a function of time. The device was operated at a voltage of 140 V across the crystal at a frequency of 1 Hz ($n = 3$; error bars correspond to SD).
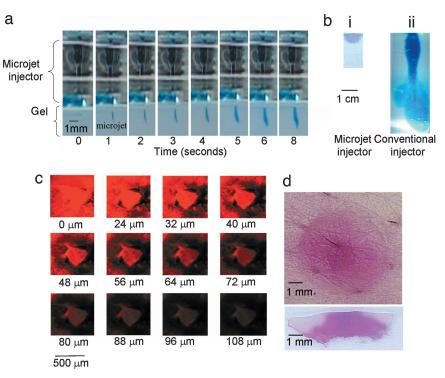
Fig. 3. Penetration of microjets into gel and human skin *in vitro*. (*a*) Penetration of microjets into 0.4% wt/vol agarose gel. Microjet was operated at 140 V and 1 Hz. Images represent stills from a video. (*bi*) Dispersion of dye after delivery by microjet for ≈30 min. (*bii*) Penetration of conventional jet into 0.4% wt/vol agarose gel delivered by Vitajet 3 (nozzle diameter, 177 μm; velocity >150 m/s) (injection volume of 35 μl). (*c*) Confocal microscopy pseudocolor images showing penetration of pulsed microjets into full-thickness human skin *in vitro* (1 μl/min, 1 Hz) (injection volume of 35 μl). (*d*) Optical images of penetration of conventional jet into human skin *in vitro*. Jets were delivered from Vitajet 3 (nozzle diameter, 177 μm; velocity >150 m/s). (*Upper*) Top view. (*Lower*) Cross-sectional view (injection volume of 35 μl).

to seven pulses. Further application of microjets does not cause substantial increase in penetration depth. Instead, the liquid delivered by microjets diffuses around the site of delivery to form a hemispherical pattern (Fig. 3*bi*). In the image shown in Fig. 3*bi*, an estimated 35 μl of liquid was delivered into the gel by prolonged application of microjets. The diameter of the hemispherical dome in Fig. 3*bi* is ≈1 cm. To put these depths into perspective, we also studied penetration of the same volume of dye solution from a conventional jet injector (Vitajet 3) into the same gel (diameter of 177 μm and velocity of >150 m/s) (Fig. 3*bii*). Compared with pulsed microjets, conventional injectors exhibited much deeper penetration (penetration depth ≫1 cm). Although these data offer a comparison between the microjet and conventional jet injectors, the absolute values of penetration depths in human skin for both injectors are different from those in gels.

The difference between microjet and conventional jet injection can also be seen in human skin. Penetration depths of microjets into human skin were confirmed *in vitro* by using sulforhodamine B (Fig. 3*c*). Confocal microscopic analysis indicated a clear region of microjet penetration up to depths of ≈100–150 μm (Fig. 3*c*, corresponding to a total delivery of 35 μl). Some diffused dye could be occasionally seen in the epidermis especially at long times; however, direct penetration of the microjet was not seen in deeper regions (>150 μm). We postulate that shallow penetration of microjets into skin is essential to mitigate pain because the density of blood vessels and nerves is less in the top 100 to 200 μm of skin. Literature studies have confirmed painless insertion of microscale objects such as microneedles into skin (19). Specifically, Kaushisk *et al.* reported that no pain was induced by insertion of microneedles (150 μm in length and 80 μm in diameter) into skin of human volunteers (19). In contrast, insertion of a 26-G hypodermic

needle caused significant pain. Note that the length and diameter of microneedles used by Kaushik *et al.* are respectively comparable to the penetration depth and diameter of microjets used in this study. For comparison purposes, the same dye was delivered into human skin by a conventional jet injector (Fig. 3*d*, Vitajet 3, volume: 35 μl, diameter: 177 μm, velocity >150 m/s). As expected, the conventional injector delivered the dye much deeper and wider into human skin. The jet penetrated deep into the dermis and a significant fraction of the liquid actually penetrated beyond the dermis (not visible in Fig. 3*d*).

Histologic evaluations of skin after microjet delivery showed no alterations in skin structure compared with untreated skin. However, it was difficult to reach a conclusion based on these data because it was not clear whether the actual injection site was captured in the histology section. The microjet itself is ≈100 μm in diameter and penetrates ≈100–150 μm into skin, thus making observation of the injection site in histology slides challenging. However, experiments with confocal microscopy provided valuable information about the tissue structure adjacent to the microinjection site (Fig. 4). This image, taken ≈15–30 min postinjection, shows the injection spot (bright circular region) and the hexagonal architecture of corneocytes around the injection spot stained by the dye, which diffused from the injection site. The architecture of corneocytes appears intact and suggests that microjet penetration has no adverse effect on tissue morphology adjacent to the injection site. The tissue structure within the actual site of microjet penetration is likely to be altered as a result of compression and shear-induced damage after microjet impact and entry. However, these alterations should be local and superficial (within the penetration region of a few hundred microns). These structural changes are expected to be reversible as a result of a combined effect of skin's elasticity, barrier recovery processes, and ultimately, epidermal turnover.
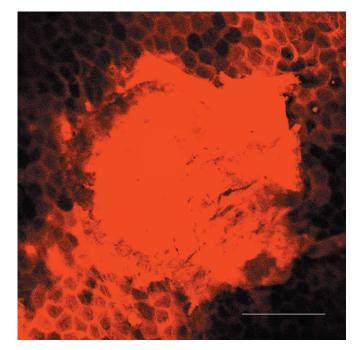
Fig. 4. Penetration of microjets into human skin *in vitro*. The image shows the intact structure of corneocytes around the injection site (bright spot at the center). The image was taken 15–30 min postinjection. (Scale bar, 200 μm.)

Quantitative estimates of microjet penetration into human skin were obtained by using radiolabeled mannitol as a tracer. For this purpose, a separate model system was designed in which isolated human epidermis was placed on the agarose gel and microjets containing a colorimetric dye and radiolabeled mannitol were delivered. Visual appearance of the dye in the gel was used to determine the number of pulses necessary to penetrate the epidermis, whereas quantitative determination of the amount of liquid delivered across the epidermis was obtained by using mannitol. A single pulse was not sufficient to penetrate the epidermis. The median number of pulses required for visible appearance of the dye across the epidermis was 48. This corresponds to a median penetration time of 48 seconds when microjets were delivered at a rate of 1 Hz. This can be reduced by up to 10-fold by increasing the microjet delivery rate to 10 Hz. During this short lag time, a negligible amount of mannitol was detected in the supporting gel. Beyond this period, the amount

of mannitol delivered increased linearly with time (Fig. 5*a*). The rate of transdermal mannitol delivery under the conditions in Fig. 5*a* is ≈ 1 μl/min.

In vivo experiments were performed in Sprague–Dawley rats to confirm systemic delivery of macromolecules by using insulin as a model drug. Microjet-delivered insulin was rapidly absorbed into systemic circulation as evidenced by a rapid decrease in blood glucose levels in a dose-dependent manner (Fig. 5*b*, closed squares, 20-min delivery; and closed circles, 10-min delivery). As a positive control, 1.5 units insulin was injected s.c. (Fig. 5*b*, open circles). Under the microjet parameters used in these experiments, it is anticipated that 2 units of insulin was delivered over 20 min, and 1 unit was delivered in 10 min (delivery of 100 units/ml insulin at ≈ 1 μl/min). A proportional reduction in glucose levels was observed when microjets were delivered for 10 and 20 min (the area above the 10-min curve in Fig. 5*b* is 56% of that above the 20-min curve). The drop in glucose levels was faster with s.c. injection. However, the area above the s.c. injection curve was comparable to the average numbers for microjet injections of 1 and 2 units, indicating the bioequivalence of the two methods. As another positive control, we also delivered 2 units insulin with a conventional jet injector (Vitajet 3, open squares). The conventional injector induced significantly rapid hypoglycemia compared with microjets, possibly as a result of deeper and wider penetration. However, jet injections were associated with significant adverse effects. Significant bleeding was observed in one animal and severe erythema was observed in another animal. Such variability in adverse effects of conventional injectors is consistent with the literature data (4). In contrast, no adverse effects (bleeding or erythema) were observed at the site of microjet injection. The site of injection itself did not have any visible mark after delivery. We attribute this to superficial penetration of microjets into skin.

The pulsed microjets described here open up new possibilities in needle-free delivery of macromolecular drugs. Compared with hypodermic needles, they offer a needle-free and patient-compliant mode of drug administration. Compared with passive transdermal patches, they allow delivery of macromolecules, provide rapid onset, and controlled, programmable, and precise dosing. Compared with conventional jet injectors, they offer shallow penetration, precise injections and potentially reduced pain and bleeding. Shallow penetration of drugs can also be advantageous for vaccination to facilitate the contact of Langerhans cells with the antigen (20, 21). Unlike conventional jet injectors, pulsed microjets use extremely small volumes and hence offer better control over delivery to superficial skin layers.
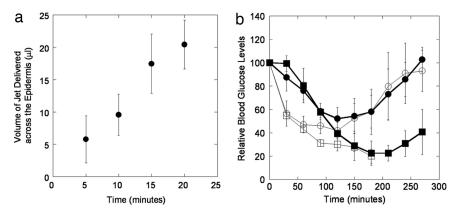

Fig. 5. Transdermal delivery mannitol in human skin *in vitro* and insulin in rat *in vivo*. (*a*) Penetration of microjets across human epidermis *in vitro* (1 μl/min, 1 Hz). Penetration increases linearly with time (*n* = 3; error bars show SD). (*b*) Delivery of insulin in Sprague–Dawley rats *in vivo* (1 μl/min, 1 Hz). Filled squares, microjets delivered for 20 min; filled circles, microjets delivered for 10 min; open circles, s.c. injection of 1.5 units; open squares, conventional jet injection (Vitajet 3, 2 units) (*n* = 3–5; error bars correspond to SD).

In its current form, the microjet injector delivers drugs at a rate of ≈1 μl/min. At a drug concentration of 20 mg/ml in the device, this flow rate translates to a delivery rate of 20 μg/min or a daily dose of ≈28 mg. This dose is sufficient for several therapeutics, for example, insulin, growth hormones, and calcitonin. This rate could be further increased by increasing the pulsing frequency and/or using multiple nozzles.

With further research focused on pharmacokinetics, safety, and device engineering, the methodology proposed here can potentially be used to deliver several drugs either in a physician's office (benchtop device) or at home (wearable device). The technology can be used as a single microjet device or can be engineered into an array of micronozzles. These devices may potentially have broad applications, including systemic, programmable delivery of drugs (for example, insulin for the management of diabetes and fentanyl for pain management), delivery of small doses in superficial layers (for example, vaccines for immunization), and precisely local delivery into epidermis (for example, antimicrobial agents for the treatment of acne and cold sores).

Materials and Methods

Microjet Generation. The pulsed microjet injector is not commercially available and was custom-made. The microjet injector consists of an electrically powered piezoelectric actuator that is used to push a plunger in an acrylic micronozzle. The displacement of the plunger ejects a microjet whose volume and velocity can be controlled by controlling the voltage and the rise time of the applied pulse. At the end of the stroke, the plunger is brought back to its original position by a compressed spring. The voltage applied to the piezoelectric crystal was varied between 0 and 140 V to generate microjets with volumes up to 15 nanoliters. The frequency of pulses was typically 1 Hz. The drug solution was filled in a reservoir, which directly feeds the solution to the micronozzle. The reservoir was maintained at slight overpressure (a small fraction of atmospheric pressure) to avoid backflow. The solution was degassed before loading in the device to minimize bubble formation in some cases. During the experiment, the injector was placed against the gel or skin so that the contact was made between the two. The volume of each microjet was measured by adding a colorimetric dye or a radiolabeled tracer (mannitol) to the solution and ejecting a known number of microjets. The ejected liquid was assayed to determine the volume of each microjet.

Measurement of Microjet Velocity. Because the entire microjet ejection occurs in a fraction of a millisecond, normal bright-field microscopy by using conventional digital cameras will not capture the ejection. Frame rates of low-noise cameras under normal operation are typically no better than 50 Hz, which is very slow to be of use. To image the microjet during injection, we developed a strobe microscopy system based on a fast light-emitting diode. The electronic shutter of the digital camera is turned on and a 0.3-μs flash from a light-emitting diode illuminates and freezes the jet in the image frame. A second flash delayed by a defined time using a digital delay generator (typically 5–10 μs) creates a second exposure on the same frame. From the double exposure, the average velocity between the flashes can be calculated, and a series of such images throughout the lifetime of the microjet can create a time-resolved record of the fluid ejection in air or gel.

Conventional Jet Injector. A commercial jet injector (Vitajet 3; Bioject Inc., Portland, OR) was used to create macroscopic jets (diameter: 177 μm and velocity >150 m/s). Vitajet 3 is a needle-free, spring-powered jet injection system that is designed for insulin delivery. The velocity of the jet was controlled by adjusting the amount of spring compression as well as the piston friction. Two plastic rings are provided with the device for increasing the spring compression. The rings can also be used together to produce maximum spring compression. Vitajet 3 has disposable piston heads and clear thermoplastic nozzles. Methods for measuring jet velocities are described elsewhere (14).

Penetration Into Gels. Agarose gels (0.4%) were used to assess penetration of microjets into solid substrates. The gel was prepared on the day of use by dissolving agarose (Sigma Aldrich Corp, St. Louis, MO) in deionized water. The microjet system was loaded with degassed saline mixed with blue dye. Microjet injections were carried out at constant frequency of 1 Hz in 0.4% agarose gel for up to 60 min. Images of microjets penetrating into gels were obtained by using a digital camera (Optronics, Goleta, CA).

Penetration Across Human Skin *in Vitro*. Human skin was obtained from the National Disease Research Interchange (NDRI, Philadelphia, PA). Epidermis was separated from full-thickness skin by using standard procedures and was placed on 0.4% agarose gel. The microjet injector was loaded with degassed saline mixed with 50 μCi/ml ^{3}H-labeled mannitol (American Radiolabeled Chemicals, Inc., St. Louis, MO) and 10 mM sulforhodamine B (Molecular Probes, Eugene, OR). Delivery across epidermis was quantified by visually confirming appearance of the dye in the gel and by measuring the amount of radioactivity in gel. For this purpose, the gel was collected at various time points in separate experiments and dissolved in Solvable tissue solubilizer (Perkin-Elmer Life and Analytical Sciences, Inc., Boston, MA). Radioactivity was counted by using Packard Tri-Carb 2100TR Scintillation Counter (Packard, Meridien, CT).

Penetration of microjets into human skin was also assessed by using confocal microscopy. Full-thickness human skin was used for this purpose. Microjet injector was loaded with 10 mM sulforhodamine B (Molecular Probes, Eugene, OR) in degassed saline. The injector was placed on the skin and activated for 5–35 min at a frequency of 1 Hz. The skin sample was mounted on glass slide and immediately frozen at −80°C until analysis to prevent diffusion of the dye. Depth and dispersion pattern of injections were visualized by using confocal microscope (Leica Microsystems, Bannockburn, IL). The samples were excited at 568 nm and emission spectra captured between 580 and 600 nm. Images were obtained in *xyz* scanning mode and captured every 2 μm from the skin surface until no appreciable fluorescence could be detected. Each image represents an average of two scans.

In Vivo Delivery of Insulin. Bioavailability of drugs by using pulsed microjet was shown in Sprague–Dawley rats using insulin as the model drug. The animals were put under anesthesia (1–4% isoflurane) and rested on their back during the procedure. The hair on the abdomen were lightly shaved for placement of the injector orifice close to the skin while avoiding any damage to skin. The orifice of the microjet was placed against the skin, thus ensuring minimal standoff distance and mimicking use of traditional jet injectors in humans. Insulin solution (Sigma–Aldrich) with activity of 100 units/ml was delivered for 10 or 20 min and blood samples collected from the tail vein before the start of injection and every 30 min thereafter. Sample collection was continued for 270 min after initiation of insulin delivery and all samples were immediately assayed for glucose level by One Touch glucose meter (LifeScan, Inc., Milpitas, CA). s.c. injection of 1.5 units served as a positive control. As an additional control, 2 units insulin was delivered using a commercial jet injector (Vitajet 3; Bioject, Inc.). All experiments were performed under protocols approved by the Institutional Animal Care and Use Committee.

1. Kermode M (2004) *Health Promot Int* 19:95–103.
2. Varmus H, Klausner R, Zerhouni E, Acharya T, Daar AS, Singer PA (2003) *Science* 302:398–399.
3. Voelker R (1999) *J Am Med Assoc* 281:1879–1881.
4. Mitragotri S (2006) *Nat Rev Drug Discov* 5:543–548.
5. Levy D, Kost J, Meshulam Y, Langer R (1989) *J Clin Invest* 83:2074–2078.
6. Mitragotri S (2005) *Nat Rev Immunol* 5:905–916.
7. Prausnitz MR, Mitragotri S, Langer R (2004) *Nat Rev Drug Discov* 3:115–124.
8. Mitragotri S, Blankschtein D, Langer R (1995) *Science* 269:850–853.
9. Prausnitz MR, Bose VG, Langer R, Weaver JC (1993) *Proc Natl Acad Sci USA* 90:10504–10508.
10. Kalia YN, Naik A, Garrison J, Guy RH (2004) *Adv Drug Deliv Rev* 56:619–658.
11. Karande P, Jain A, Mitragotri S (2004) *Nat Biotechnol* 22:192–197.
12. Doukas AG, Kollias N (2004) *Adv Drug Deliv Rev* 56:559–579.
13. Zhang I, Shung KK, Edwards DA (1996) *J Pharm Sci* 85:1312–1316.
14. Schramm J, Mitragotri S (2002) *Pharm Res* 19:1673–1679.
15. Bremseth DL, Pass F (2001) *Diabetes Technol Ther* 3:225–232.
16. Schram-Baxter J, Mitragotri S (2004) *J Control Rel* 97:527–535.
17. Fletcher D, Palenkar D (2001) *Appl Phys Lett* 78:1933–1935.
18. Fletcher D, Palenkar D, Huie P, Miller J, Marmor M, Blumenkranz M (2002) *Arch Ophthalmol* 120:1206–1208.
19. Kaushik S, Hord AH, Denson DD, McAllister DV, Smitra S, Allen MG, Prausnitz MR (2001) *Anesth Analg* 92:502–504.
20. Hammond SA, Guebre-Xabier M, Yu J, Glenn GM (2001) *Crit Rev Ther Drug Carrier Syst* 18:503–526.
21. Jakob T, Udey MC (1999) *Adv Dermatol* 14:209–258; discussion 259.